Applied Energy 283 (2021) 116282

Contents lists available at ScienceDirect

Applied Energy

journal homepage: www.elsevier.com/locate/apenergy

Optimal midterm peak shaving cost in an electricity management system using behind customers' smart meter configuration

Agustín A. Sánchez de la Nieta [a,*], Iliana Ilieva [b], Madeleine Gibescu [a], Bernt Bremdal [b,c], Stig Simonsen [d], Eivind Gramme [d]

[a] Energy & Resources group, Copernicus Institute of Sustainable Development, Utrecht University, The Netherlands
[b] Smart Innovation Norway, Norway
[c] The Arctic University of Norway, Narvik, Norway
[d] Skagerak Energi AS, Norway

ARTICLE INFO

Keywords:
Electricity management system
Energy storage system
Local load
Decentralised PV production
Peak shaving service
Prosumer
Stochastic mixed-integer linear problem

ABSTRACT

This paper analyses a local electricity system (LES) comprising photovoltaic production (PV), a connection to the distribution network, local loads and an energy storage system (ESS). Given the flexibility of the ESS, the LES can provide a peak shaving service (PSS) to the grid operator based on the actual monthly power tariff. This paper proposes a stochastic mixed-integer linear programming problem that maximises the expected operating profit of the LES midterm. Assuming a behind customers' smart meter configuration, income is derived from selling the energy of prosumers to other external electrical areas. If the costs are higher than the income, the net profit will be negative, i.e. a net loss. The cost component of the objective function can be reduced through the management of local resources and by providing PSS to the distribution network operator to minimise the power cost of the monthly power tariff. The model is tested for 720 h (considering a month of 30 days) in three cases: (i) without PV and ESS; (ii) with PV and ESS, where losses are 0%; (iii) with PV and ESS, where losses are 18%. Due to the monthly power tariff, the net loss of the LES is reduced through the optimal management of local resources when the ESS losses are lower than 18%. To assess seasonal implications about the LES, the 12 months of the year are also tested. The month of October indicated the highest peak shaving, while the lowest peak shaving depended on the ESS losses.

1. Introduction

The electric power grid faces challenges related to the growing share of distributed energy resources (DERs (see the table of acronyms Table 1)). As renewable energy sources increase their presence in distributed systems, energy storage systems (ESSs) and electric vehicles are rapidly penetrating markets. Hence, the impact of ESSs and electric vehicles on power grids can be lessened through local electricity management systems. Consumers and prosumers who choose to be flexible regarding their non-time-critical consumption production needs can help alleviate grid challenges. In particular, local energy consumers and prosumers can sell their flexible consumption/production loads to different interested actors within the power system. The flexible loads can be utilised for congestion management and grid operation, among others. In this way, local flexibility providers can make a profit on energy flexibility sales or reduce their electricity bills. Flexible consumption and production can be facilitated through well-designed local markets that provide proper incentives for the participation of local market actors.

The increasing penetration of intermittent power generation boosts the higher deployment of flexibility resources. In this respect, local electricity markets (LEMs) strive to provide flexibility-associated benefits for all those connected to local grid parties. To encourage local energy production and active prosumer participation, the local market should offer its participants attractive contracts and have the technology, business and optimisation tools needed to guarantee the fair and efficient utilisation of local resources. In this context, the local electricity system (LES) characteristics (such as grid configuration, types of DERs and local market actors) are particularly important. This paper demonstrates optimal local electricity management with peak shaving service (PSS), referring to a microgrid-based local market structure specified within the E-REGIO project [1].

* Corresponding author.
E-mail addresses: agustinsnl@gmail.com (A.A.S. de la Nieta), iliana.ilieva@smartinnovationnorway.com (I. Ilieva), M.Gibescu@uu.nl (M. Gibescu), bernt.bremdal@smartinnovationnorway.com (B. Bremdal), stig.simonsen@skagerakenergi.no (S. Simonsen), eivind.gramme@skagerakenergi.no (E. Gramme).

https://doi.org/10.1016/j.apenergy.2020.116282
Received 25 June 2020; Received in revised form 23 October 2020; Accepted 16 November 2020
Available online 3 December 2020

Table 1
Acronym.

BCSM	Behind customers' smart meter.
DERs	Distributed energy resources.
DSO	Distribution system operator.
ESS	Energy storage system.
LEM	Local electricity market.
LES	Local energy system.
LL	Local load.
LSO	Local system operator.
MILP	Mixed-integer linear programming.
NC	Distribution network.
PSS	Peak shaving service.
PV	Photovoltaic production.
RTE	Round trip efficiency of the ESS.
SESP	Smart energy service provider.
SMILP	Stochastic mixed-integer linear programming.
SOE	State of energy.
WM	Wholesale market.

1.1. Literature review

Various options for managing energy resources locally are discussed in the literature. In particular, the focus has been on local markets, grid services and electricity management systems.

- Local markets
  European regulation was analysed in [2] and enablers of local flexibility markets were identified. An optimisation problem (mixed-integer linear programming [MILP]) was proposed in [3] to satisfy the necessity for the required flexibility from distribution system operators. Furthermore, research in [4] presented the development of short-term decision support models for aggregators who sell electricity to prosumers and buy the excess of local generation. The two-stage stochastic mixed-integer linear programming problem (SMILP) allowed simulating the aggregator model over two months.
  The role of ESSs in local markets was addressed in [5]. The authors created an agent-based simulation study of local peer-to-peer electricity trading in a community. The study reflected on two local market scenarios, i.e. with and without local community storage. The aim was to procure electricity directly from local renewable generation. Accordingly, [5] concluded an increased local market efficiency impact associated with the utilisation of community storage. In the study of [6], energy storage was used to reduce system congestion cost caused by the two peaks by sending cost-reflective economic signals, where a new charging and discharging strategy based on binary search method was defined. Hence, a locational marginal pricing method was created for energy storage. Although the work presented in [7] does not deal with local markets, two relevant (for the local markets' context) strategies of PV power producers without an ESS were presented, where the PV producers could participate in the day-ahead and intraday markets and the imbalance markets.
  The work presented by [8] envisioned a microgrid environment, in which consumers and prosumers trade at the local market to keep profits within the community.
  Within research on LEMs, studies have focused on different LEM configurations considering the distribution system operators (DSOs) and residential customers. As presented in [9], DSOs can be beneficiaries of contracts and services through local market structures. Furthermore, co-simulated distribution networks and peer-to-peer energy trading platforms were discussed in [9]. Residential customers were analysed in [10] via experimental analysis. Next, centralised and decentralised analysis of local markets were addressed in [11]. The centralised approach was used as a benchmark of [11], where the national market operator optimally scheduled the bids of generators. The decentralised approach was modelled using the Stackelberg leadership model, which, by clearing local market procedures can be solved in simultaneous or sequential modes.
  Peer-to-peer energy trading is currently a popular area of research. A review on peer-to-peer and community-based markets was introduced in [12]. Peer-to-peer trading for prosumers in a residential building in London was tested in [13] with a degree of system flexibility provided by battery storage. To manage the uncertainty, a peer-to-peer local electricity market for trading energy and uncertain power with demand having power flexibility was developed in [14], while a prediction–integration model was implemented in [15] for a prosumer in continuous double auction-based peer-to-peer.
- Grid services and energy management systems
  The primary grid services are peak shaving, congestion management and frequency reserve. A techno-economic analysis was introduced in [16] for the peak shaving and frequency containment reserve that battery storage could provide in Norway. [16] conducted analyses considering balancing prices, grid charges, degradation of batteries and opportunity investment costs. Another approach for testing the ESS was adopted in the form of the robust optimisation of system congestion management [17]. An ESS in Madeira, Portugal, was presented in [18], where arbitrage, self-sufficiency, peak shaving and energy back up were co-optimised.
  The peak shaving service for grid operation was analysed in [19], which focused on vehicle-to-grid technology (V2G). A review of peak shaving was presented in [20], which focused on the importance of peak load shaving, peak shaving using ESS, peak shaving based on electric vehicles and peak shaving using demand-side management.
  A pivotal part of grid services is energy management, which is applied for DERs and loads. [21] studied DERs sharing in the context of peak shaving and load balance, where the aggregation of DERs was carried in energy and capacity markets and consumer contributions were evaluated through an energy sharing scheme. Other investigations have focused on specific modelling characteristics. Load smoothing and peak shaving based on load forecasting through artificial neural networks were analysed in [22]. A multi-agent system framework was applied in the peak shaving and valley filling potential of PV production with an ESS for a high-rise residential building [23].

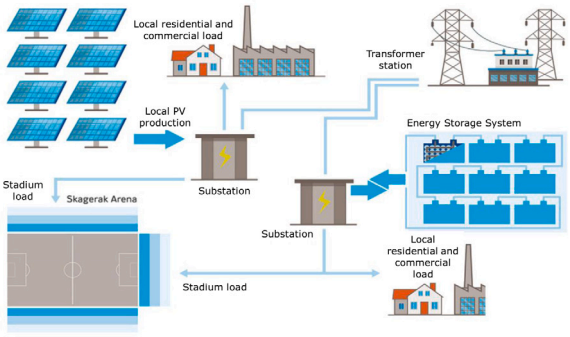

Fig. 1. Illustration of the LES.

1.2. Aims and contributions

This study provides a preliminary analysis of a new energy trading platform operated by a smart energy service provider (SESP) or a local system operator (LSO). In the core of the energy trade is a local energy system (LES) that includes PV production, an ESS, local load (LL) and a connection with the distribution network (NC) as shown in Fig. 1.

Table 2
Nomenclature.

Indices and sets	
b ($\mathcal{B}$)	Index (set) related to blocks of the power (energy per hour) tariffs.
j ($\mathcal{J}$)	Index (set) related to LLs.
p ($\mathcal{P}$)	Index (set) related to periods.
s ($\mathcal{S}$)	Index (set) related to scenarios.
Parameters	
$C^{NET^{ESS}}$	Cost tariff of the energy flow from the NET to the ESS [€/kWh].
$C^{NET^{LOAD}}$	Cost of the energy flow from the NET to the LOAD [€/kWh].
$C^{PV^{SHED}}$	Cost of the energy flow from the PV to be SHED [€/kWh].
ESS^{LIMIT}	Maximum energy injected into the energy storage system [kWh].
$load_{j,p,s}$	Consumption of LL j in scenario s and period p [kWh].
$losses$	Losses that happen in the ESS, whose energy stored is lost in physical and chemical processes.
M^{flow}	Maximum energy limit per hour [kWh/h].
$M^{energyflow}$	Maximum energy limit [kWh].
$peak_b^{LIMIT^{MAX}}$	Power (energy per hour) size of block b of cost-quantity curve for the maximum power (energy per hour) per month kWh/h [kWh/h].
$p_{p,s}^{PV}$	PV production of PV panels in scenario s and period p [kWh].
q_b^{min}	Summation of power (energy per hour) blocks from block $b = 1$ to block b-1 [kWh/h].
SOE^{MAX}	Maximum energy of the SOE [kWh].
SOE^{MIN}	Minimum energy of the SOE [kWh].
$tariff_b^{POWER}$	Tariff of block b paid by the LL for the maximum power (energy per hour) of the time frame analysed [€/kWh/h].
$tariff^{PROSUMER}$	Price or tariff of the energy flow from the PV and ESS to the NET, prosumer tariff [€/kWh].
γ	Efficiency of charging/discharging the ESS.
$\lambda_{p,s}^{WM}$	Day-ahead wholesale market price in scenario s and hour p [€/kWh].
ρ_s	Probability of scenario s.
Decision variables	
$cost_{p,s}$	Total cost of the local energy system in scenario s and period p [€].
$cost_{p,s}^{NET}$	Cost of the NET in scenario s and period p [€].
$cost^{POWER}$	Cost associated with the maximum power (energy per hour) for the time frame [€].
$cost_{p,s}^{PV}$	Cost of all flows of PV production in scenario s and period p [€].
$ESS_{j,p}^{LOAD}$	Energy flow from the ESS to the LL j, in period p [kWh].
ESS_p^{NET}	Energy flow from the ESS to the NET in period p [kWh].
$I_{p,s}^{PROSUMER}$	Incomes of the energy flow from the PV or ESS to the NET in scenario s and period p, as a prosumer [€].
$LIMIT^{PS}$	Energy per hour as a limit of the power (energy per hour) flow from the NET [kWh/h].
$NET_{p,s}^{ESS}$	Energy flow from the NET to the ESS in scenario s and period p [kWh].
$NET_{j,p,s}^{LOAD}$	Energy flow from the NET to the local LOAD j, in scenario s and period p [kWh].
$peak_b^{LIMIT}$	Power (energy per hour) of block b used for the maximum power (energy per hour) per month kWh/h [kWh/h].
PF	Profits of the local energy system [€].
$pf_{p,s}$	Total profits in each scenario s and period p [€].
PV_p^{ESS}	Energy flow from the PV to the ESS in each period p [kWh].
$PV_{j,p}^{LOAD}$	Energy flow from the PV to the local LOAD j in each period p [kWh].
PV_p^{NET}	Energy flow from the PV to the NET in each period p [kWh].
$PV_{p,s}^{SHED}$	PV shed in each scenario s and period p [kWh].
SOE_p	State of energy level in period p [kWh].
$Total_{p,s}^{NET}$	Total energy comes from the NET in scenario s and period p [kWh].
η_p	Losses of the stored energy in period p [kWh].
Binary variables	
dc_p	1 if the ESS charges, 0 when ESS discharges in period p.
l_b	1 if the block b was completely used, 0 otherwise in block b.
$net_{p,s}^{flow}$	1 if the energy flow goes from the network to the local electricity system, 0 otherwise in scenario s and period p.
u_b	1 if the block power (energy per hour) tariff b is active, 0 otherwise in block b.

The E-REGIO LES is a facility located in the south of Norway. The actual installations of local resources are: stadium load, residential and commercial loads, rooftop PV panels in the stadium, an energy storage system (ESS), and the distribution network operator (Skagerak Energi AS).

This paper proposes a mathematical model, stochastic mixed-integer linear problem (SMILP), to analyse the described LES. The analysis of the LES targets the energy management system of a centralised local market considering the ambitions of the E-REGIO project. In this context, electricity market proposed within E-REGIO is a local market concept for trading products and services such as peak shaving, local energy surplus, local renewable production and flexibility provided by the local ESS. The implications of the ESS are also tested regarding its efficiency, which is tested with a 0 and 18% of losses. The 18% of loss is associated with the actual loss of the ESS.

More specifically, this paper is focused on the smart energy management system of local resources of the E-REGIO pilot site in Norway. Hence, the smart energy management system is part of the business case for a local energy system behind the customer's smart meter (BCSM).

This model, together with the measured data, provides relevant information for practical future implementation of the E-REGIO market concept as a local smart grid and electricity market, in other European jurisdictions. Moreover, the analysis of peak shaving service requires data over a period of at least one month to resemble the actual power tariff of the distribution network. Hence, the time frame of the optimisation model was adjusted for 720 h (30 days multiplied by 24 h) as average month hours. This power limit tariff characteristic based on the actual Norwegian market serves as a clear contribution to the scheduling of local resources but also limits the SMILP problem.

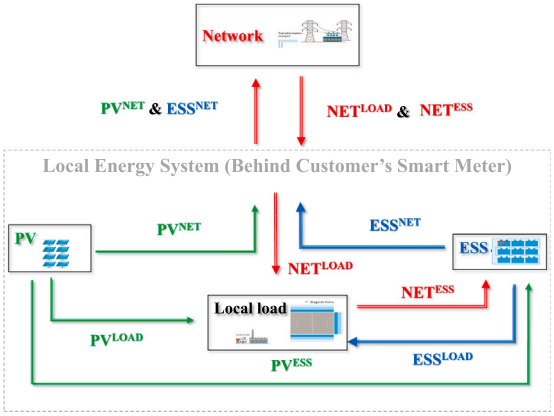

Fig. 2. Illustration of the energy flows.

Accordingly, the contributions of this paper are threefold as noted below.

- A new smart energy management system, focused on managing local resources from an economic point of view. The main objective is to maximise the midterm net profits, while the midterm peak shaving service minimises the distribution network costs of the local energy system, thereby promoting a more independent LES.
- A novel stochastic programming model that allows for evaluating the novel smart energy management system for the Norwegian E-REGIO pilot, following the actual tariff design. The proposed optimisation model provides relevant feedback for future business models of the E-REGIO LEM.
- Realistic simulations of monthly operations for one full year. This annual analysis captures the stochastic nature of demand, PV generation and wholesale market prices. By capturing seasonal variations, the study provides pivotal information for the practical implementation of the E-REGIO LEM in the current and future Norwegian context.

1.3. Paper organisation

The remainder of this paper is structured as follows. The assumptions are introduced in Section 2. Section 3 describes mathematical formulation, while Section 4 presents data and results of the pilot study. Section 5 presents the main conclusions from the results provided in Section 4.

2. Assumptions

Several assumptions and considerations were included in the study as noted below.

- Any month of the year comprising 30 days was considered; this provided for 30 days multiplied by 24 h (720 h), which allowed for the comparison between months.
- Power (kW) was considered energy per hour kWh/h. Moreover, the time step resolution of simulations was one hour, indicating the importance of kW and kWh/h.
- The NC did not have power congestion problems, although the model included the energy per hour flow limit (presented by kWh per hour).
- All loads considered in the paper were local loads, i.e. the local consumption that happens in the LES.
- Midterm optimisation (optimisation for a time frame of 720 h (one month) with hourly time step resolution) presented difficulty for formulating scenarios. Hence, months from the preceding six years were selected as scenarios classified according to month; e.g. January group included all the January months in the six preceding years.
- The actual ESS showed losses equal to 18% and was compared with a case without losses.
- The PV and ESS power capacity are not included in the model because the facilities are predefined by pilot set-up.
- In the text, LL is used as equivalent to LOAD and NC to NET; LL and NC are used in the text, while LOAD and NET are used in the mathematical model.

Finally, with reference to the Norwegian pilot, the envisioned energy flows are illustrated in Fig. 2. The energy flows are as follows: (i) the ESS can inject energy into the LL and NC; the ESS can also charge energy from the PV producer and NC; (ii) the LL energy is only consumed by participants in the form of residential and commercial loads; (iii) the PV can send energy to the ESS, LL and NC; (iv) the NC allows energy to be injected into the LES and the distribution system.

3. Mathematical formulation

In this section, a novel optimisation model based on two-stage stochastic programming is introduced to determine the optimal profile of local resources considering midterm peak shaving cost.

The first-stage decision variable set represents *here-and-now* decisions. The first-stage variables represent the first interest. The second-stage decision variable set includes the *wait-and-see* decisions, which drive recourse decisions to a specific realisation regarding the random variables. This mathematical formulation follows a model formulated as node-variable; therefore, the formulation does not need non-anticipativity constraints. The first-stage decision variables do not have a scenario index s, while the second-stage decision variables depend on the scenario index s. The nomenclature used in the mathematical model is presented in Table 2.

Fig. 3 shows the objective function of the optimisation problem, which maximises the profits, subject to seven block constraints.

The problematic constraints of this mathematical model are divided into seven blocks: expected profit, PV energy flows, ESS energy flows and SOE, LL energy balance, NC energy flow, peak shaving and energy flow directions.

The mathematical model needs to satisfy all the constraints to be feasible. The development of the mathematical model follows the energy flow concept, as shown in Fig. 4.

The interactions between elements follow the diagram of Fig. 4. The PV can inject energy into the LL, ESS, NC, and shed, while the ESS can inject energy into the LL and NC. The NC can inject into the LL and ESS. These interactions between the PV, ESS and NC will depend on the costs and incomes, trying to maximise the profit of the LES. There are two important decisions through the binary variables. These are charge or discharge the ESS through the dc_p binary variable and inject energy into the LES or NC through the $net_{p,s}^{flow}$ binary variable.

3.1. Objective function

The objective function is presented in (1), which maximises the total expected profit PF (2); hence, the total expected profit may be positive (net profit) and negative (net loss). The total expected profit comprises income and costs. The LES only has an income when it sells the local production to the wholesale market (WM) through the NC as a prosumer. Local production can be derived from PV production and ESS. However, costs are derived from energy injected into the LES, which is used by the LL and ESS. This energy injected by the NC into the LES has an equivalent cost to the prices of the WM. Due to lower

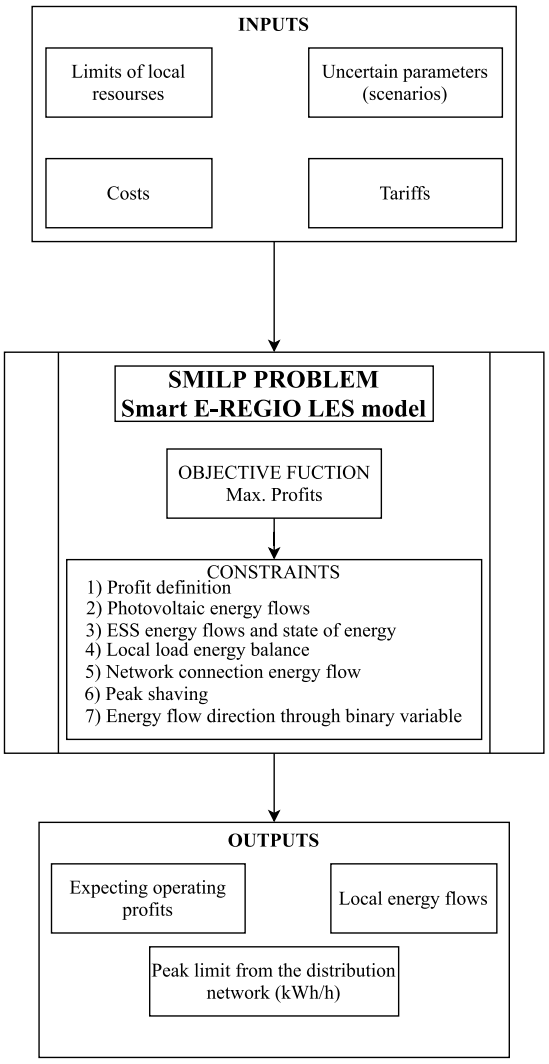

Fig. 3. Diagram of the simulation process.

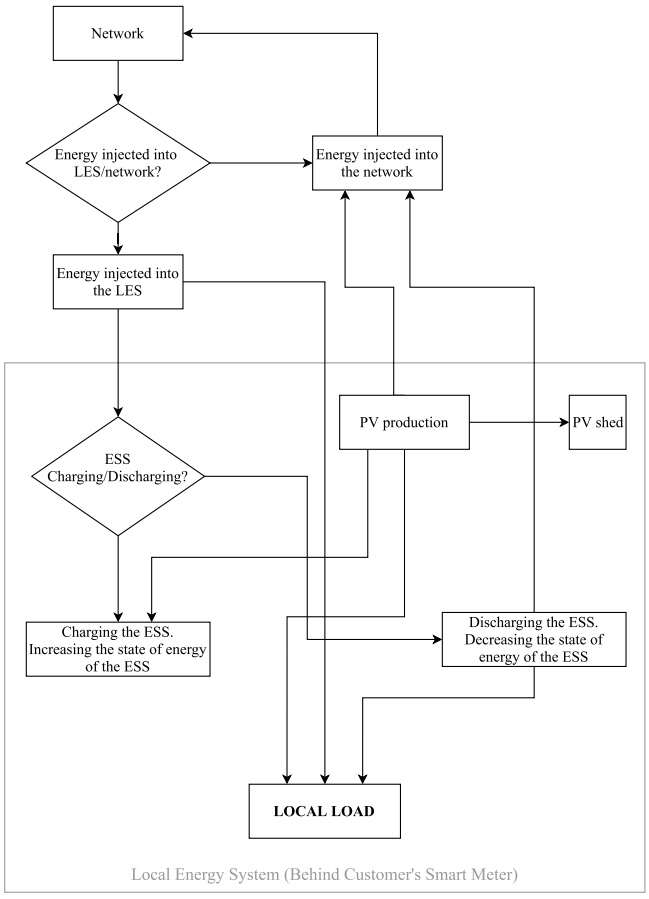

Fig. 4. Flow chart of the control logic in the optimal management of the LES.

PV production compared with the LL and energy from the NC charged in the ESS, the total expected profit will be a net loss (costs are higher than the income). The objective function then maximises the income and minimises the costs, subject to all the constraints.

Maximise PF. (1)

3.2. Expected profit constraints

The total operating profits PF (2) are defined as the expected profit minus the power cost for the time frame of one month.

The expected profits per scenario and period (3) are prosumer incomes minus the costs associated with the energy. Then, the prosumer incomes (4) are the wholesale prices plus the tariff as prosumer multiplied by the energy injected into the WM through the connection. This injected energy represents the energy flows from the PV and ESS. The energy flows of the LES are shown in Figs. 2 and 4. Regarding the costs of (5), these include costs associated with the WM and PV production shed costs. The costs associated with the WM (6) are the wholesale prices plus the grid tariff of the NC multiplied by the energy flow that goes from the NC to the ESS. Furthermore, a similar cost is set for the LL, with the wholesale prices and grid tariff of the NC multiplied by the LL as the second part of (6). A PV cost (7) is considered when it is shed. The LES uses the PV shed mechanism only when it is required for effecting an energy balance. The PV shed cost is the marginal cost associated with the PV shed.

Eq. (8) defines the power cost. This equation represents different blocks of power with different tariffs. Once the first energy block of maximum energy per hour is used, the second block starts being used. The first energy block has a higher cost than the second energy block. The formulation of this cost has two parts. The block cost is the block tariff multiplied by the binary variable. This variable shows whether the block was used l_b and the total energy of the block. The second part of (8) is the cost of the last block activated, where part of the energy block was used. Then, the second part of (8) is the block power tariff multiplied by the energy used in that block. See Fig. 5.

$$PF = \sum_{s\in S}(\rho_s \cdot \sum_{p\in P} pf_{p,s}) - cost^{POWER}; \tag{2}$$

$$pf_{p,s} = I^{PROSUMER}_{p,s} - cost_{p,s}; \forall p \in P, \forall s \in S; \tag{3}$$

$$I^{PROSUMER}_{p,s} = (\lambda^{WM}_{p,s} + tariff^{PROSUMER}) \cdot (PV^{NET}_{p} + ESS^{NET}_{p}); \forall p \in P, \forall s \in S; \tag{4}$$

$$cost_{p,s} = cost^{NET}_{p,s} + cost^{PV}_{p,s}; \forall p \in P, \forall s \in S; \tag{5}$$

$$cost^{NET}_{p,s} = (\lambda^{WM}_{p,s} + C^{NET^{ESS}}) \cdot NET^{ESS}_{p,s} + (\lambda^{WM}_{p,s} + C^{NET^{LOAD}}) \cdot \sum_{j\in J} NET^{LOAD}_{j,p,s}; \forall p \in P, \forall s \in S; \tag{6}$$

$$cost^{PV}_{p,s} = C^{PV^{SHED}} \cdot PV^{SHED}_{p,s}; \forall p \in P, \forall s \in S. \tag{7}$$

$$cost^{POWER} = \sum_{b\in B}\left(tariff^{POWER}_{b} \cdot l_b \cdot peak^{LIMIT^{MAX}}_{b} + tariff^{POWER}_{b} \cdot peak^{LIMIT}_{b}\right). \tag{8}$$

3.3. Photovoltaic energy flows constraints

Eq. (9) evaluates the energy flow that goes from the PV to the NC, LL, ESS and PV shed. The summation of all PV energy flows is equal to the scenarios of PV production, being an uncertain parameter.

$$PV_{p}^{NET} + \sum_{j\in\mathcal{J}} PV_{j,p}^{LOAD} + PV_{p}^{ESS} + PV_{p,s}^{SHED} = p_{p,s}^{PV};\quad \forall p \in \mathcal{P}, \forall s \in \mathcal{S}. \tag{9}$$

3.4. Energy storage system energy flows and state of energy constraints

Another type of energy flow is ESS energy flow (10), which sees energy from the ESS sent to the LL and NC. The summation of flows from the ESS to the NC and LL must be equal to or lower than the state of energy (SOE) in that period.

Eq. (11) is the SOE SOE_p. It is equal to the SOE in period $p-1$ plus the energy charged in the ESS from the PV and NC. When the ESS discharges, this energy is injected into the NC and/or LL [24]. Moreover, this SOE considers losses, which are defined in (12) as a percentage of the SOE. Finally, this SOE has upper and lower limits (13).

$$ESS_{p}^{NET} + \sum_{j\in\mathcal{J}} ESS_{j,p}^{LOAD} \leq SOE_p; \forall p \in \mathcal{P}; \tag{10}$$

$$SOE_p = SOE_{p-1} + \frac{PV_{p}^{ESS}}{\gamma} + \frac{NET_{p,s}^{ESS}}{\gamma} - ESS_{p}^{NET}\cdot\gamma - \sum_{j\in\mathcal{J}} ESS_{j,p}^{LOAD}\cdot\gamma - \eta_p; \forall p \in \mathcal{P}, \forall s \in \mathcal{S}; \tag{11}$$

$$\eta_p = SOE_p \cdot losses; \forall p \in \mathcal{P}; \tag{12}$$

$$SOE^{MIN} \leq SOE_p \leq SOE^{MAX}; \forall p \in \mathcal{P}. \tag{13}$$

3.5. Local load energy balance constraints

Constraint (14) evaluates the balance between generation and demand as LL. The generation that satisfies the LL $load_{j,p,s}$ comes from the PV $PV_{j,p}^{LOAD}$, NC $NET_{j,p,s}^{LOAD}$ and ESS $ESS_{j,p}^{LOAD}$. Due to the LL is uncertain, the model mitigates that uncertainty with the energy imported from the NC. Hence, the variable $NET_{j,p,s}^{LOAD}$ depends on the scenario, index s. Then, this variable $NET_{j,p,s}^{LOAD}$ belongs to the second-stage, the wait-and-see decisions.

$$PV_{j,p}^{LOAD} + NET_{j,p,s}^{LOAD} + ESS_{j,p}^{LOAD} = load_{j,p,s}; \quad \forall j \in \mathcal{J}, \forall p \in \mathcal{P}, \forall s \in \mathcal{S}. \tag{14}$$

3.6. Network connection energy flow constraints

The network connection energy flow constraints, (15) and (16), show the energy flows and total energy associated with the NC, respectively. To avoid problems with the LL, the NC provides energy mitigating the uncertainty of the LES. Then, the energy injected into the LES from the NC as shown in Fig. 4 is decided with the $NET_{j,p,s}^{LOAD}$ and $NET_{p,s}^{ESS}$ variables, which depend on the scenario, index s, for mitigating the uncertainty of the LES. Those two variables will define the maximum energy per hour (kWh/h) injected into the LES, being the $LIMIT^{PS}$. It is considered as the peak shaving concept because the cost of the power related to the tariff $tariff_{b}^{POWER}$ will reduce the kWh/h injected into the LES from the NC. The constraints of this section are related to quantifying the energy from the NC.

$$\sum_{j\in\mathcal{J}} NET_{j,p,s}^{LOAD} + NET_{p,s}^{ESS} \leq LIMIT^{PS}; \forall p \in \mathcal{P}, \forall s \in \mathcal{S}; \tag{15}$$

$$Total_{p,s}^{NET} = \sum_{j\in\mathcal{J}} NET_{j,p,s}^{LOAD} + NET_{p,s}^{ESS}; \forall p \in \mathcal{P}, \forall s \in \mathcal{S}. \tag{16}$$

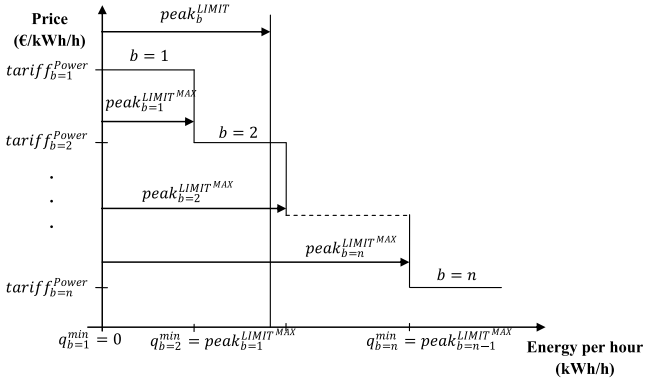

Fig. 5. Conceptual view of the price-energy per hour for the power tariff.

3.7. Peak shaving constraints

Peak shaving is pivotal to the current study. The equations consider the peak limit $LIMIT^{PS}$ that is required to satisfy the power needed in the LES. The peak shaving is the difference between the scenarios of LL and the limit of peak shaving that satisfies all scenarios in the highest LL of one period with the conditions of PV and ESS. Fig. 5 shows how the power tariff is modelled and the meaning of the parameters and variables.

The peak limit Eqs. (17)–(19) define the blocks of power that the power tariffs are divided into. Moreover, these equations evaluate the block where the total energy injected into the LES from the NC occurs. We developed these block tariffs following the definition of blocks as in [25], with selected differences. Eq. (17) limits the power of the block to the maximum power of the b block. The binary variable u_b is activated only in one block; then (18) fixes the summation of the binary variable u_b per block b to 1. However, the previous blocks of the active block are considered for the power cost. Eq. (19) is needed to derive the power and cost of used blocks. This equation evaluates the power blocks that were activated. Then, the summation of the previous active power blocks known through the binary variable l_b is equal to the activated power block u_b multiplied by the summation of power blocks q_{b}^{min}. Eq. (19) determines the binary variable l_b used in (8) for the $cost^{POWER}$. The total power is evaluated in (20); it is the summation per block of the power required of the active block plus the summation of previous power blocks.

$$0 \leq peak_{b}^{LIMIT} \leq u_b \cdot peak_{b}^{LIMIT^{MAX}}; \forall b \in \mathcal{B}; \tag{17}$$

$$\sum_{b\in\mathcal{B}} u_b = 1; \tag{18}$$

$$\sum_{b\in\mathcal{B}} \left(l_b \cdot peak_{b}^{LIMIT^{MAX}}\right) = \sum_{b\in\mathcal{B}} \left(u_b \cdot q_{b}^{min}\right); \tag{19}$$

$$LIMIT^{PS} = \sum_{b\in\mathcal{B}} \left(peak_{b}^{LIMIT} + u_b \cdot q_{b}^{min}\right). \tag{20}$$

3.8. Energy flow direction through binary variable constraints

Eqs. (21)–(29) are the limits of energy flows and peak shaving. Some of these limits also require binary variables such as dc_p and $net_{p,s}^{flow}$. The dc_p binary variable decides whether the ESS charges or discharges and the $net_{p,s}^{flow}$ binary variable decides whether the NC injects energy into the LES or the WM.

$$0 \leq LIMIT^{PS} \leq M^{flow}; \tag{21}$$

$$0 \leq ESS_{p}^{NET} \leq ESS^{LIMIT} \cdot (1 - dc_p); \forall p \in \mathcal{P}; \tag{22}$$

$$0 \leq ESS_{j,p}^{LOAD} \leq ESS^{LIMIT} \cdot (1 - dc_p); \forall j \in \mathcal{J}, \forall p \in \mathcal{P}; \tag{23}$$

$$0 \leq NET_{p,s}^{ESS} \leq ESS^{LIMIT} \cdot dc_p; \forall p \in \mathcal{P}, \forall s \in \mathcal{S}; \tag{24}$$

$$0 \leq NET_{p,s}^{ESS} \leq ESS^{LIMIT} \cdot net_{p,s}^{flow}; \forall p \in \mathcal{P}, \forall s \in \mathcal{S}; \quad (25)$$

$$0 \leq PV_{p}^{ESS} \leq ESS^{LIMIT} \cdot dc_{p}; \forall p \in \mathcal{P}; \quad (26)$$

$$0 \leq NET_{j,p,s}^{LOAD} \leq M^{energyflow} \cdot net_{p,s}^{flow}; \forall j \in \mathcal{J}, \forall p \in \mathcal{P}, \forall s \in \mathcal{S}; \quad (27)$$

$$0 \leq ESS_{p}^{NET} \leq ESS^{LIMIT} \cdot (1 - net_{p,s}^{flow}); \forall p \in \mathcal{P}, \forall s \in \mathcal{S}; \quad (28)$$

$$0 \leq PV_{p}^{NET} \leq ESS^{LIMIT} \cdot (1 - net_{p,s}^{flow}); \forall p \in \mathcal{P}, \forall s \in \mathcal{S}. \quad (29)$$

Finally, selected positive decision variables not defined previously are $cost_{p,s}$, $cost_{p,s}^{NET}$, $cost^{POWER}$, $cost_{p,s}^{PV}$, $I_{p,s}^{PROSUMER}$, $LIMIT^{PS}$, $PV_{j,p}^{LOAD}$, $PV_{p,s}^{SHED}$, $Total_{p,s}^{NET}$ and η_p.

4. Case study and results

4.1. Data

The E-REGIO LES is a real facility located in the south of Norway. Herein, we introduce all the parameters needed for our simulations, representing data from the actual installations, the applicable distribution network operator (Skagerak Energi AS) tariffs and wholesale market prices from Nord Pool [26].

There are two types of parameters, i.e. certain and uncertain. The costs considered in the model are $C^{NET^{ESS}} = C^{NET^{LOAD}} =$ €0,0205/kWh from September to April and €0,0186/kWh for the remaining months of the year. To avoid problems when there is an excess of PV production that cannot be injected into the network, the PV production can be shed with a cost $C^{PV^{SHED}} =$ €0,05/kWh. There is also a power cost $tariff_{b}^{POWER}$, which is associated with peak shaving. $tariff_{b}^{POWER}$ is a power tariff per blocks. $peak_{b=1}^{LIMIT^{MAX}} =$ 200 kWh/h and the cost is €6,35/kWh/h. Once the 200 kWh/h is paid to €6,35/kWh/h, the rest of power has a cost of €5,54/kWh/h. Then, q_{b}^{min} has two blocks. The first block is 0 and the second is 200 kWh/h. Then, the limit of the network connection is $peak_{b=1}^{LIMIT^{MAX}} = M^{FLOW}$ = 3000 kWh/h. As such, there are only two blocks as it is shown in Fig. 6. A tariff for the income as a prosumer is $tariff^{PROSUMER}$ equal to €0,0186/kWh.

The ESS has different parameters. Its power limit is 800 kW, it is ESS^{LIMIT} = 800 kWh per hour and the ESS loss is $losses$ = 0,18, meaning that it has 18% of losses or a round trip efficiency (RTE) of 82%. Hence, two cases were analysed for the ESS. These two cases involved PV production and an ESS with a loss of 18% (real losses of the ESS) and with PV production and an ESS with a loss of 0%. The maximum and minimum limits of the SOE of the ESS are $SOE^{MAX} =$ 1000 kWh and $SOE^{MIN} = 0{,}2 \cdot SOE^{MAX}$ kWh, which is 20% of the maximum SOE. We consider a $\gamma = 1$, which is 100% efficiency when the energy is charged or discharged in the ESS.

The uncertain parameters are the $load_{j,p,s}$, $p_{p,s}^{PV}$ and $\lambda_{p,s}^{WM}$. The uncertainty of these parameters is considered using scenarios. Due to the time frame needed for deriving the power cost of 720 h, the scenarios were created using real data for each month of previous years. Then, the data from the preceding six years (from 2013 to 2018) of the LL and WM prices [26] were used as scenarios. However, the PV panel facilities were only recently installed (PV power capacity of 800 kWp) in Norway. Thus, we could only use simulations that included selected measures of the location. The scenarios for PV production were created using this information. Based on these simulations, a yearly simulation hour per hour was found for all 8760 h. Hence, each hour per month (from 1 to 24 h) was adjusted to a truncated normal distribution. Following on, simulations per hour of each month were run. As previously noted, six PV scenarios were selected. Due to using the monthly data of the six preceding years, the number of scenarios per uncertain parameter was decided as six. To illustrate these three uncertain parameters, Figs. 7–9 show the scenarios for each of them, respectively. Each colour of the Figs. 7–9 represents each scenario of the uncertain parameters.

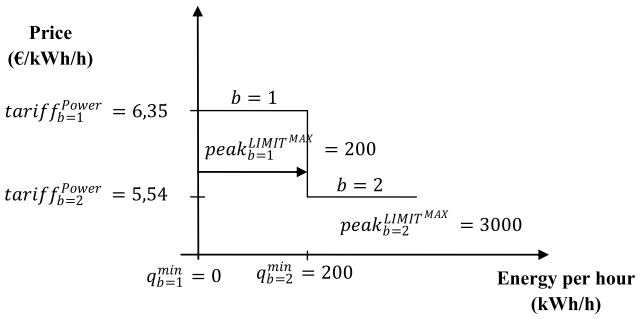

Fig. 6. Price-energy per hour for the power tariff of the case study.

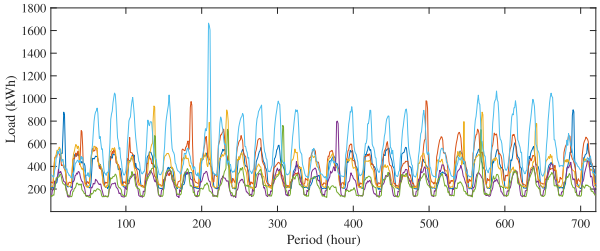

Fig. 7. Scenarios of the LL of the LES in July.

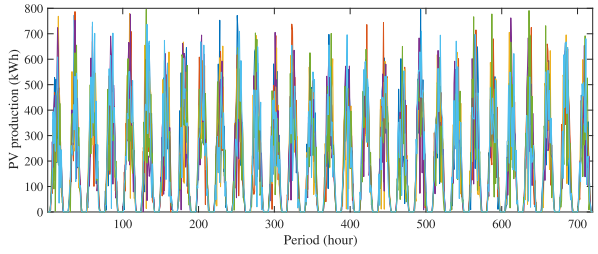

Fig. 8. Scenarios of the PV production of the LES in July, 2019.

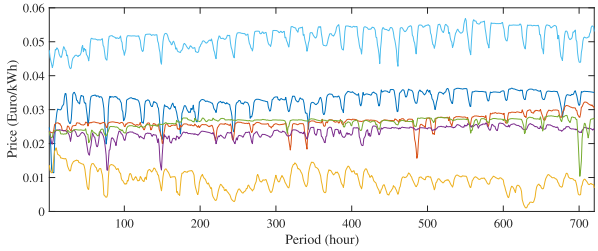

Fig. 9. Scenarios of the wholesale electricity prices of the LES in July, 2019.

The three uncertain parameters were then combined in a tree. Hence, a tree was used to create the scenarios. The scenario tree, similar to [27], is composed of i) 6 scenarios of the LL, ii) 6 scenarios of the PV production and iii) 6 scenarios of the WM prices. This provided a total number of scenarios equal to $6 \cdot 6 \cdot 6 = 6^3 = 216$. If there were 216 total scenarios, the probability per scenarios as equiprobable was ρ_s = 0,0046.

4.2. Results

This Section 4.2 has two parts. The first introduces one month (July 2019) and the second the annual results of three cases.

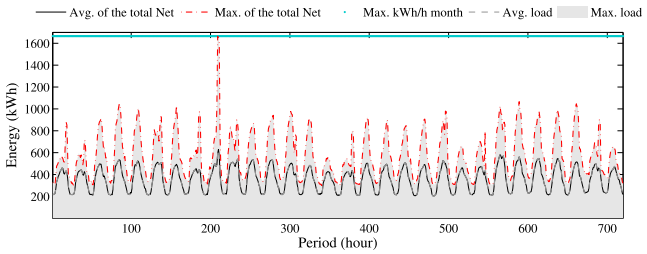

Fig. 10. Case 1: average and maximum of the total imported energy from the network, the maximum kWh/h per month and the average and maximum of the LL in July, 2019.

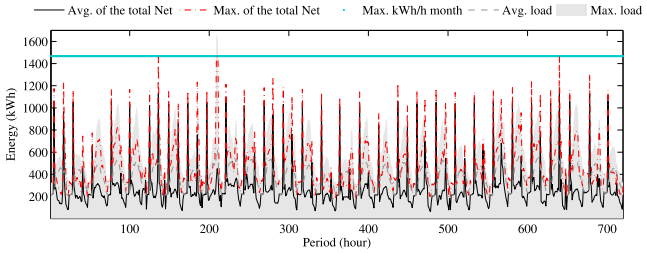

Fig. 11. Case 2: average and maximum of the total imported energy from the network, the maximum kWh/h per month and the average and maximum of the LL in July, 2019.

To establish an analysis with a clear comparison of the results, the simulations of a reference case were conducted. This reference case, case 1, was the LES without PV production and an ESS. This reference case allowed for a comparison with the PV production and ESS cases. The ESS can have losses of 0% (case 2) and 18% (case 3). The case 3 is presented because the actual loss of the ESS is 18%. The case 2 and case 3 are equivalent to 100% of RTE and 82% of RTE, respectively.

The leading case study is the case 3, but the case 1 and case 2 allow comparing the actual case (case 3) with the reference of the previous situation to install the PV and the ESS (case 1) and if the ESS is perfect (case 2).

4.2.1. Case 1: LES without PV production and an ESS July 2019

This case 1 is how the LES has been working so far. Fig. 10 shows the maximum of energy imported, without peak shaving because there are not PV production and an ESS.

Fig. 10 presents a maximum of total Net that will be the maximum kWh/h per month in the hour 209, equal to 1.666 kWh/h. Moreover, the maximum load is equal to the maximum of the total Net. Hence, the power cost is 1.666 kWh/h multiplied by €5,54/kW is equal to €9229,64.

4.2.2. Case 2: LES with PV production and an ESS (0% of loss) July 2019

This case 2 has three peaks in Fig. 11, in the 136, 211 and 640 h. The average of the total Net is more volatile than in case 1 because the PV and ESS change the profile of the energy imported from the NC.

A maximum of power was required to satisfy the peak consumption in 136, 209 and 640 h, where the maximum LL in the 209 h could be 1.666 kWh/h and the energy imported from the NC could be 1.467 kWh/h. Hence, peak shaving reduced the power in July by 199 kWh/h and multiplied by €5,54/kW, and this peak shaving reduced the power cost by €1.102.

Due to the ESS having loss of 0%, the maximum Net to the ESS in Fig. 12 has only peaks because the energy is only used to charge the ESS and does not need to compensate the loss of the ESS.

The PV production does not need to compensate the loss of the ESS, as shown in Fig. 13. The total PV profile follows the profile of the PV scenarios presented in Fig. 8.

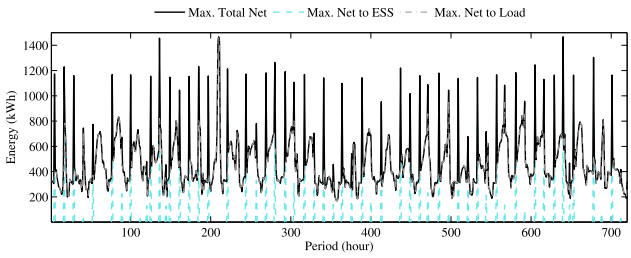

Fig. 12. Case 2: the maximum total network energy injected into the LES, the maximum energy from the network to the ESS and maximum energy from the network to the LL in July, 2019.

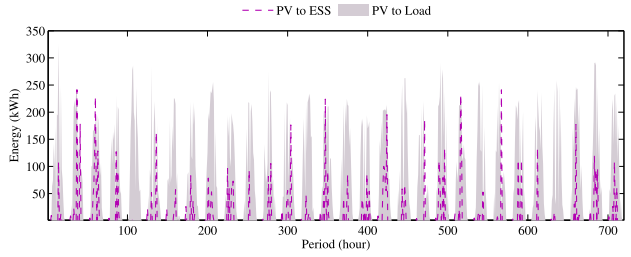

Fig. 13. Case 2: the PV energy flow towards ESS and LL in July.

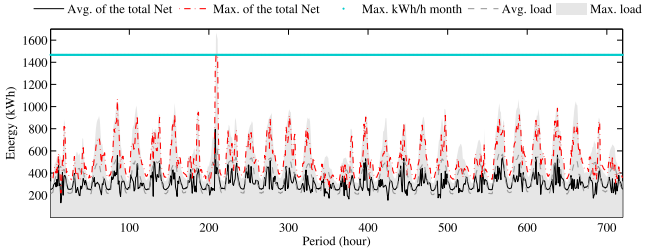

Fig. 14. Case 3: average and maximum of the total imported energy from the network, the maximum kWh/h per month and the average and maximum of the LL in July, 2019.

4.2.3. Case 3: LES with PV production and an ESS (18% of loss) July 2019

The main results presented are related to the energy imported into the LES, maximum power kWh/h per month, LL, energy imported to charge the ESS and satisfy the LL and the PV production to be injected into the ESS and LL.

Fig. 14 presents the behaviour of the model in July, 2019. The maximum kWh/h in July (720 h) was 1.467 kWh/h. This maximum was required to satisfy the peak consumption in hour 209, where the maximum LL in this hour could be 1.666 kWh. Hence, peak shaving reduced the power in July by 199 kWh/h. Multiplied by €5,54/kW, this peak shaving reduced the power cost by €1.102.

Additionally, the average of the total net (injected energy into the LES from the distribution network) was lower for the peak periods and higher for the off-peak periods. During this time, the injected energy considering the PV and ESS was flatter than without the PV and ESS.

Fig. 15 shows the energy flows from the NC that can go to the LL and ESS. As shown in Fig. 15, the energy flow from the NC to the LL had a similar maximum values profile to the maximum total energy injected from the NC to the LES. The main differences arose from the peak and off-peak periods as illustrated in Fig. 14.

We also observed an energy flow from the NC to the ESS when there was no PV production as shown in Fig. 15. This energy flow happened to compensate for the losses of the ESS and the minimum SOE of the ESS as 20% of the maximum SOE. There were some peaks of the energy flow from the PV to the ESS that mitigated selected NC peaks. Moreover, the energy flow from the PV to the LL was higher

Table 3
The profits, maximum kWh/h and PS of the three cases; case 1: without PV production and an ESS; case 2: with PV production and an ESS with losses = 0%; case 3: with PV production and an ESS with losses = 18%.

	Case 1		Case 2			Case 3		
Month	PF (€)	Max. kWh/h	PF (€)	Max. kWh/h	PS (kWh/h)	PF (€)	Max. kWh/h	PS (kWh/h)
1	−25.767	1.137	−24.618	961	176	−26.825	1.043	93
2	−25.858	1.395	−23.813	1.043	352	−25.611	1.062	334
3	−25.858	1.395	−23.813	1.043	352	−25.612	1.058	337
4	−24.672	1.730	−23.788	1.565	165	−25.271	1.565	165
5	−22.128	1.691	−21.092	1.436	255	−22.484	1.436	255
6	−21.234	1.660	−20.702	1.503	157	−22.038	1.503	157
7	−21.498	1.666	−20.531	1.467	199	−21.881	1.467	199
8	−21.042	1.476	−19.723	1.277	198	−21.070	1.280	196
9	−23.223	1.562	−21.889	1.250	311	−23.504	1.280	282
10	−25.066	1.691	−23.043	1.299	392	−24.627	1.312	379
11	−27.327	1.608	−25.780	1.342	266	−27.434	1.352	256
12	−24.561	1.125	−23.393	941	184	−25.484	1.012	113
Total	−288.235	18.134	−272.184	15.126	3.008	−291.840	15.368	2.766

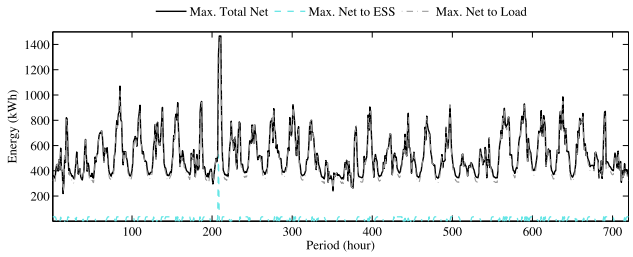

Fig. 15. Case 3: the maximum total network energy injected into the LES, the maximum energy from the network to the ESS and maximum energy from the network to the LL in July, 2019.

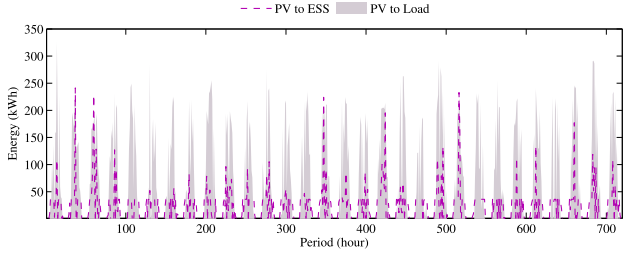

Fig. 16. Case 3: the PV energy flow towards ESS and LL in July, 2019.

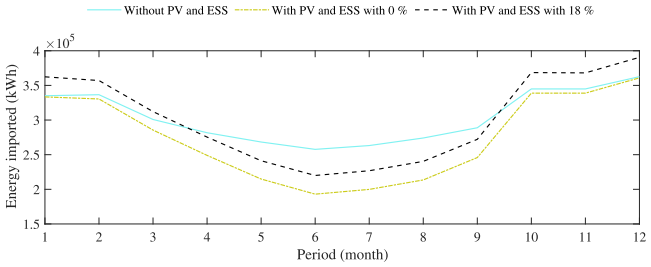

Fig. 17. Monthly energy imported from the distribution network without PV production and ESS, with PV production and ESS with losses of 0% and with PV production and ESS with losses of 18%.

than to the ESS as shown in Fig. 16. This happened because the energy flow from the PV to the LL, unlike the ESS, did not experience losses.

The operation of the LES with LL, PV production, ESS and a connection to the distribution network had a profit equal to €−21.881 and the maximum kWh/h was 1.467 kWh/h in July. Here, the profits were negative (net loss); this infers a cost that arises because of the energy imported from the NC and PV shed.

4.2.4. Annual results with and without energy storage system losses

Comparisons between all the months of the entire year, profits, maximum kWh/h and the peak shaving in the three cases are presented in Table 3.

During the summer months, the negative profit (net loss) were lower compared to the rest of the year. The summer months had lower consumption and higher PV production; however, some summer months also showed a higher maximum kWh/h use. This higher maximum also occurred in the spring months.

From the total annual results, the highest profits (the lowest net loss) were detected in the presence of PV production and an ESS with losses = 0%, where peak shaving was 3.008 kWh/h for the entire year. However, higher losses reduced profits (higher net loss) and peak shaving. Reduced profits infer higher costs; consequently, the LES with PV production and an ESS with losses = 18% increased the total costs of the system. Furthermore, the peak shaving was lower, from 3.008 kWh/h to 2.766 kWh/h. These higher costs were derived from the ESS, which had a minimum level of energy for the entire day, i.e. the minimum SOE SOE^{MIN} constraint.

The lowest negative profit (net loss) in all cases was observed for August, while the lowest max. kWh/h occurred in December. Following this trend, the highest peak shaving happened in October. However, the lowest peak shaving occurred in different months, depending on the losses incurred. For a perfect ESS (losses = 0%), this was the case in June, while with losses of 18% this was in January.

The total energy injected into the LES from the distribution network is presented in Fig. 17. The lowest annual energy imported happened when the loss of the ESS was 0%. When the ESS had losses equal to 18%, more energy was imported than in cases without PV and ESS during the months of autumn and winter, while the energy imported was lower in summer and spring periods as shown in Fig. 17. The total energy imported for the three cases without PV and ESS was 3.658.657 kWh; for PV and ESS with losses = 0% this was 3.303.969 kWh and for cases with PV and ESS with losses = 18% total energy was 3.634.560 kWh. Notwithstanding the higher energy imported in the autumn and winter periods, the case with PV and ESS with losses = 18% had the lower total annual energy imported than the case without PV and ESS.

5. Conclusions

A two-stage stochastic programming model was presented in this paper. The optimisation model scheduled the resources of a local energy system, such as PV production and an ESS behind a connection with a distribution network. Moreover, this paper considered the minimisation of the power-dependent connection cost for which a peak shaving service was provided. Hence, our conclusions are as follows.

- Local resources introduce more flexibility in the LES. This flexibility supports higher independence from the distribution network. An LES is a clear example of a new business approach for companies interested in managing local resources and providing services to the grid operator.
- The efficiency of the ESS is pivotal for providing flexibility and improving the profitability of the business case.
- The peak shaving service is not sufficient for achieving a profitable PV–ESS system based on the current pricing and regulatory framework. Hence, more research is needed to enable the provisioning of other ESS services.
- The PV local resource is the most beneficial local resource for the LES because the PV power produces local and low-cost electricity. The oversized ESS capacity also allows to install more PV power capacity and provide more services, as needed by the distribution grid.

As the ESS has been installed with the purpose of future research projects, future work will be devoted to multi-ownership of local resources in LES and new configurations different to BCSM. An interesting extension will be to mix multi-ownership, new configurations, multi ESS services, and mid-term forecasting time series.

CRediT authorship contribution statement

Agustín A. Sánchez de la Nieta: Conceptualization, Formal analysis, Investigation, Methodology, Software, Writing - original draft, Writing - review & editing. **Iliana Ilieva:** Conceptualization, Writing - review & editing. **Madeleine Gibescu:** Conceptualization, Writing - review & editing. **Bernt Bremdal:** Conceptualization, Writing - review & editing. **Stig Simonsen:** Conceptualization. **Eivind Gramme:** Conceptualization.

Declaration of competing interest

The authors declare that they have no known competing financial interests or personal relationships that could have appeared to influence the work reported in this paper.

Acknowledgement

The E-REGIO project (2017–2020) received funding from the ERA-Net Smart Grids Plus initiative, with support from the European Union's Horizon 2020 Research and Innovation program under grant agreement No 646039.

References

[1] E-Regio project. Smart Community Markets, https://www.eregioproject.com/.
[2] Minniti S, Haque N, Nguyen P, Pemen G. Local markets for flexibility trading: Key stages and enablers. Energies 2018;11(11):3074.
[3] Olivella-Rosell P, Bullich-Massagué E, Aragüés-Peñalba M, Sumper A, Ottesen SØ, Vidal-Clos J-A, Villafáfila-Robles R. Optimization problem for meeting distribution system operator requests in local flexibility markets with distributed energy resources. Appl Energy 2018;210:881–95.
[4] Ottesen SØ, Tomasgard A, Fleten S-E. Prosumer bidding and scheduling in electricity markets. Energy 2016;94:828–43.
[5] Mengelkamp E, Garttner J, Weinhardt C. The role of energy storage in local energy markets. In: 2017 14th international conference on the European energy market (EEM). IEEE; 2017, p. 1–6.
[6] Yan X, Gu C, Li F, Wang Z. LMP-Based pricing for energy storage in local market to facilitate pv penetration. IEEE Trans Power Syst 2018;33(3):3373–82.
[7] de la Nieta AAS, Paterakis NG, Gibescu M. Participation of photovoltaic power producers in short-term electricity markets based on rescheduling and risk-hedging mapping. Appl Energy 2020;266:114741.
[8] Mengelkamp E, Gärttner J, Rock K, Kessler S, Orsini L, Weinhardt C. Designing microgrid energy markets: A case study: The brooklyn microgrid. Appl Energy 2018;210:870–80.
[9] Ilieva I, Gramme E. DSOs as beneficiaries of innovative contracts and services, facilitated through local electricity market structures. AIM; 2019.
[10] Mengelkamp E, Schönland T, Huber J, Weinhardt C. The value of local electricity-a choice experiment among german residential customers. Energy Policy 2019;130:294–303.
[11] Le Cadre H. On the efficiency of local electricity markets under decentralized and centralized designs: a multi-leader stackelberg game analysis. CEJOR Cent Eur J Oper Res 2019;27(4):953–84.
[12] Sousa T, Soares T, Pinson P, Moret F, Baroche T, Sorin E. Peer-to-peer and community-based markets: A comprehensive review. Renew Sustain Energy Rev 2019;104:367–78.
[13] Zepter JM, Lüth A, del Granado PC, Egging R. Prosumer integration in wholesale electricity markets: Synergies of peer-to-peer trade and residential storage. Energy Build 2019;184:163–76.
[14] Zhang Z, Li R, Li F. A novel peer-to-peer local electricity market for joint trading of energy and uncertainty. IEEE Trans Smart Grid 2019;11(2):1205–15.
[15] Chen K, Lin J, Song Y. Trading strategy optimization for a prosumer in continuous double auction-based peer-to-peer market: A prediction-integration model. Appl Energy 2019;242:1121–33.
[16] Ahčin P, Berg K, Petersen I. Techno-economic analyis of battery storage for peak shaving and frequency containment reserve. In: 2019 16th international conference on the european energy market (EEM). IEEE; 2019, p. 1–5.
[17] Yan X, Gu C, Zhang X, Li F. Robust optimization-based energy storage operation for system congestion management. IEEE Syst J 2019.
[18] Hashmi MU, Pereira L, Bušić A. Energy storage in madeira, Portugal: co-optimizing for arbitrage, self-sufficiency, peak shaving and energy backup. In: 2019 IEEE milan powertech. IEEE; 2019, p. 1–6.
[19] Aziz N, Shah MA, Mehmood MU. Vehicle to grid (v2g) for peak shaving: New trend, benefits, and issues. Int J Comput Commun Netw 2019;1(2):27–37.
[20] Uddin M, Romlie MF, Abdullah MF, Halim SA, Kwang TC, et al. A review on peak load shaving strategies. Renew Sustain Energy Rev 2018;82:3323–32.
[21] Wang J, Zhong H, Wu C, Du E, Xia Q, Kang C. Incentivizing distributed energy resource aggregation in energy and capacity markets: An energy sharing scheme and mechanism design. Appl Energy 2019;252:113471.
[22] Chapaloglou S, Nesiadis A, Iliadis P, Atsonios K, Nikolopoulos N, Grammelis P, Yiakopoulos C, Antoniadis I, Kakaras E. Smart energy management algorithm for load smoothing and peak shaving based on load forecasting of an island's power system. Appl Energy 2019;238:627–42.
[23] Wang Y, Liu L, Wennersten R, Sun Q. Peak shaving and valley filling potential of energy management system in high-rise residential building. Energy Procedia 2019;158:6201–7.
[24] de la Nieta AAS, Tavares TA, Martins RF, Matias JC, Catalão JP, Contreras J. Optimal generic energy storage system offering in day-ahead electricity markets. In: 2015 IEEE eindhoven powertech. IEEE; 2015, p. 1–6.
[25] de la Nieta AAS, Contreras J, Muñoz JI, O'Malley M. Modeling the impact of a wind power producer as a price-maker. IEEE Trans Power Syst 2014;29(6):2723–32.
[26] Nord Pool AS. https://www.nordpoolgroup.com/historical-market-data/.
[27] de la Nieta AAS, Contreras J, Catalao JP. Optimal single wind hydro-pump storage bidding in day-ahead markets including bilateral contracts. IEEE Trans Sustain Energy 2016;7(3):1284–94.